White Paper IX

Some Initial Comparisons Between the Russian Research on

"The Nature of Torsion" and the Tiller Model of

"Psychoenergetic Science": Part I

By:

William A. Tiller Ph.D.

The William A. Tiller Foundation

Introduction

At the 2009 ISSSEEM Conference at the Westin, Westminster Hotel in Colorado, Dr. Claude Swanson presented an excellent review of recent progress on subtle energy research in Russia based upon his upcoming book[1] (the term "subtle energies was first used in print by this author in 1977[2] and more fully expressed in 1993[3]). The initial principles of this Russian work were laid down by the astrophysicist, Dr. Nikolai Kozyrev about 50 years ago. He postulated that it relates to the flow of time and gravitational effects via particle spin, rotation and entropy production: (1) The D-space electric substance spin properties were postulated to produce a space curvature contribution to Einstein's Relativity Equations and thus a contribution to spacetime gravitational effects. The Russian workers implied that this could be a possible source for "dark matter and dark energy", (2) Kozyrev found that an evaporating acetone-filled container placed immediately adjacent to a small mass, suspended by an asymmetric torsion pendulum held inside a vacuum chamber, actually repelled the small mass. He called this right-handed torsion, S_R, or time-emission. When, instead, he used a source of negative entropy production, such as the freezing of water to produce ice, it caused an attraction of the small mass. He called this left-handed torsion, S_L, or time-absorption. And (3) Kozyrev also used a flat circular disc, suspended from its center via a vertical fiber fastened at the other end to the inside top of the vacuum chamber as a torsion pendulum. He placed the entropy generating source outside the vacuum chamber and immediately adjacent to the fiber support mount on the inside of the vacuum chamber. For a positive entropy production source, the suspended flat disk rotated in a clockwise direction as viewed from the top of the fiber. For a negative entropy production source, the disk rotated in a counter-clockwise direction as viewed from the top of the fiber.

These three experimental considerations of Kozyrev should serve as a good initial test of Tiller's Psychoenergetic Science modeling framework to provide a plausible explanation for such results. That is the main goal of this White Paper, so let us proceed towards that end.

A. From the Tiller Model Perspective, Where Does An Electric Matter Particle's Spin Come From?

For any electric matter particle, whether quark, nucleon, photon, atom, etc., my working hypothesis is that a de Broglie, particle-pilotwave plus deltron construct must form first as discussed somewhat in White Paper VII[4] and applied to the dark matter and dark energy question in White Paper VI[5]. This construct with a deltron cloud is illustrated in Figure 1 where it is understood that the system

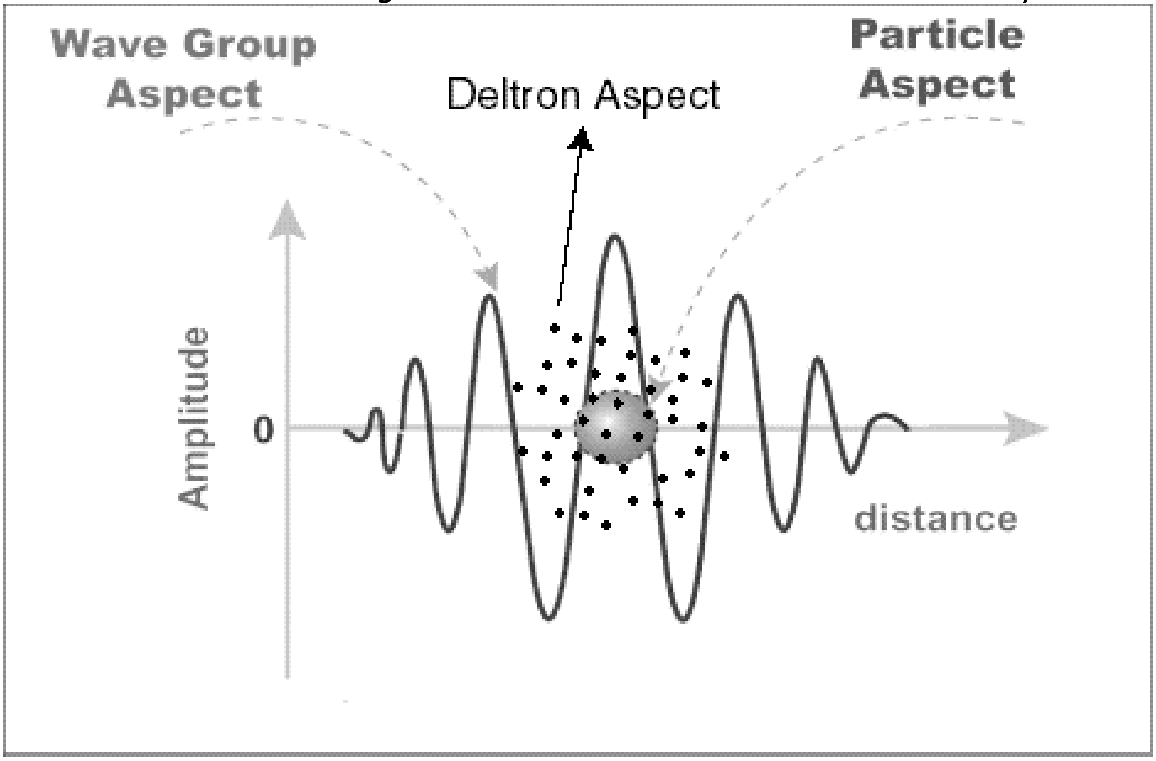

Figure 1. A schematic illustration of a D-space particle surrounded by its de Broglie pilot wave with the two being bound together via a deltron cloud so that they can collectively move to the right at velocity, v_p.

has cylindrical symmetry about the distance axis. Most simply, taking the electric particle to be an electron, its trajectory along the x-axis at velocity, v_p, constitutes an electric current flow in the reverse direction so that, by the right-hand rule, a circulating magnetic field in the counter clockwise direction is induced in the plane perpendicular to the x-axis. Since the de Broglie pilot-wave is of magnetic information wave origin, it will rotate in the $\underline{B}$-field of the medium. It is this rotation that generates the property of spin in the de Broglie particle-deltron-pilotwave-system. If the net magnetic monopole charge of the pilot wave is of a negative nature, then the pilot wave rotation will be in the counter clockwise direction constituting a positive magnetic current which, in turn, generates an axial electric field that increases the velocity of the electron to $v'_p > v_p$. If, on the other hand, the net magnetic monopole charge of the pilot wave is reversed then the pilot wave rotation will be in the counter-clockwise direction constituting a negative magnetic current and ultimately generating a slowing down of the electron. It is presumed that some type of friction force from interactions with the surrounding medium will lead to some stable electron velocity, v_p*, and some stable pilot wave spin rate.

B. Negative Energy States Are Not Necessarily Non-Physical

In reference 5, pp 5, 6, it was proposed that negative energy states in nature could be understood as bound-states within some thermodynamic potential well where, for a dimer molecule, the zero of energy for an atom is chosen as the dissociation energy for its dimer molecule. Figure 2 gives us a potential energy vs. separation distance of the atoms in the Be_2 dimer along with the first ten bound vibrational energy levels. Of course, as usual, here the zero of energy is taken to

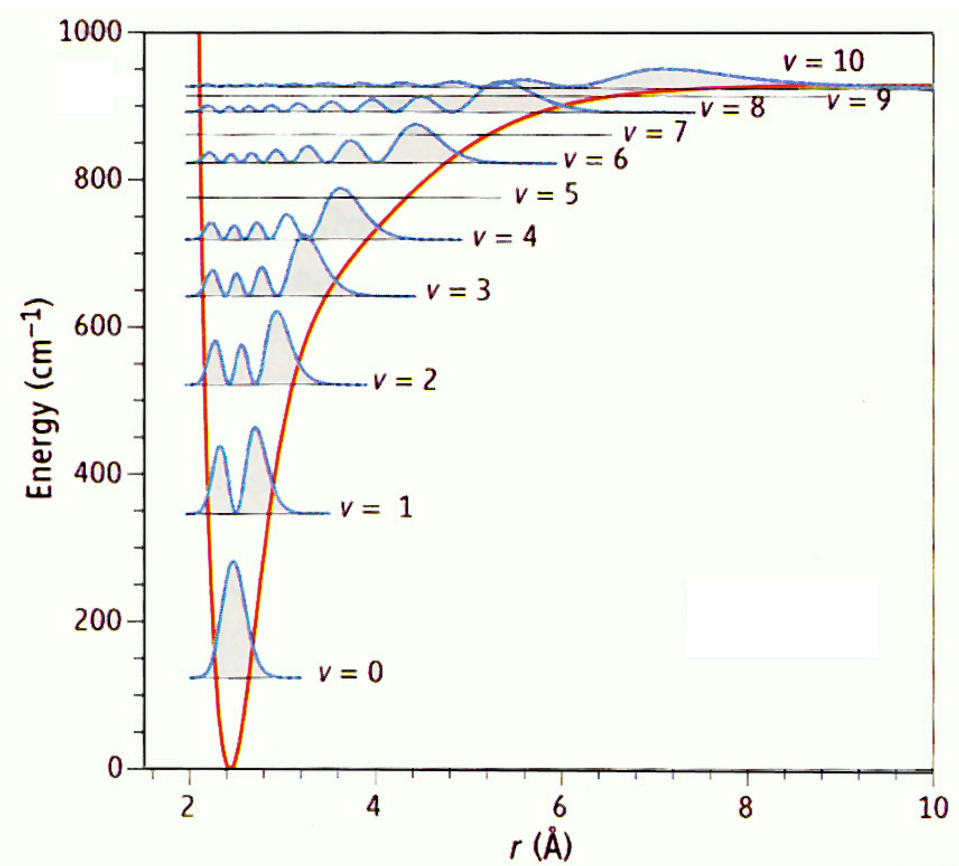

Figure 2. Potential energy for the Be_2 dimer as a function of Be atom separation distance, r, plus the first ten bound vibrational energy levels.

occur at the potential energy minimum for the dimer whereas, for the monomer, it should be taken at Figures 2's dissociation energy and all ten of these vibrational levels will have negative energies relative to the monomer Be (beryllium) zero of energy.

Figure 3a is an energy band diagram that the Tiller model utilizes

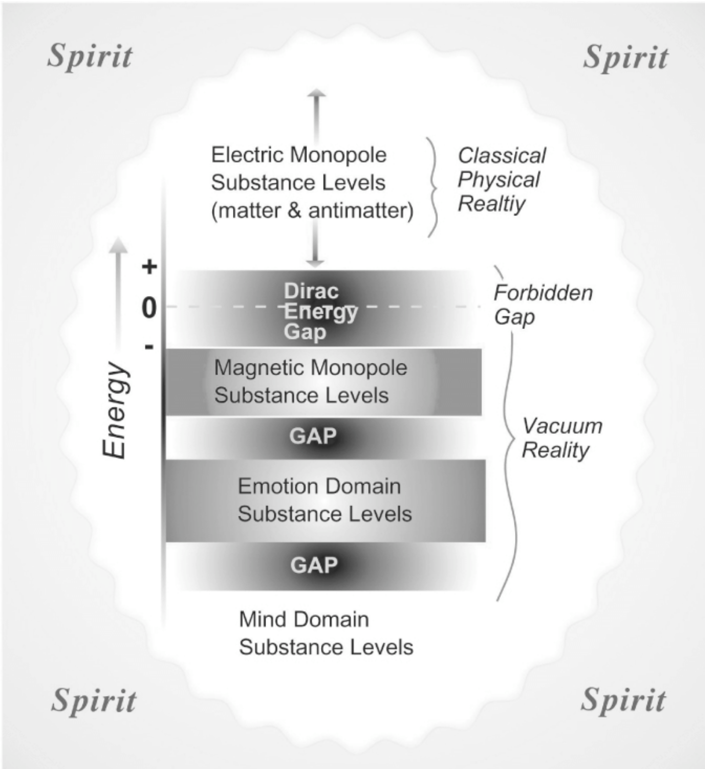

Figure 3a. An energy level diagram embracing both classical physical substances and "unseen" vacuum substances.

for its qualitative multidimensional considerations. Figure 3b is an expansion of Figure 3a to indicate both (1) the presence of an all-encompassing high spirit domain thermodynamic potential well for all the lower dimensional substances and (2) that the reference frame (RF) coordinates for these negative energy substances are all of the frequency ν_j-type. The reference frame for the positive energy substance, electric atoms, molecules, etc., is x_4 = spacetime. This author labels both the positive energy electric charge substance and the negative magnetic energy charge substance as parts of what we call physical reality.

C. <u>The Tiller Model Perspective on Where Do Gravitation, Dark Matter and Dark Energy Effects Come From?</u>

In pages 7, 8 of reference 5, this topic has been fairly completely addressed. In brief, negative energy substance means negative mass substance. Thus, magnetic information wave substance, even though invisible to our conventional instrumentation, can interact with its own kind to produce a gravitational force proportional to the product M_1M_2 = a positive number when both M_1 and M_2 are of the same sign, either both plus or both minus. Likewise, magnetoelectric (ME) photons will curve space much as do EM photons although the sign of the curvature should be reversed unless the space curvature depends on the square of the ME photon energy. Thus, this is the Tiller Model candidate for both Dark Energy and Dark Matter.

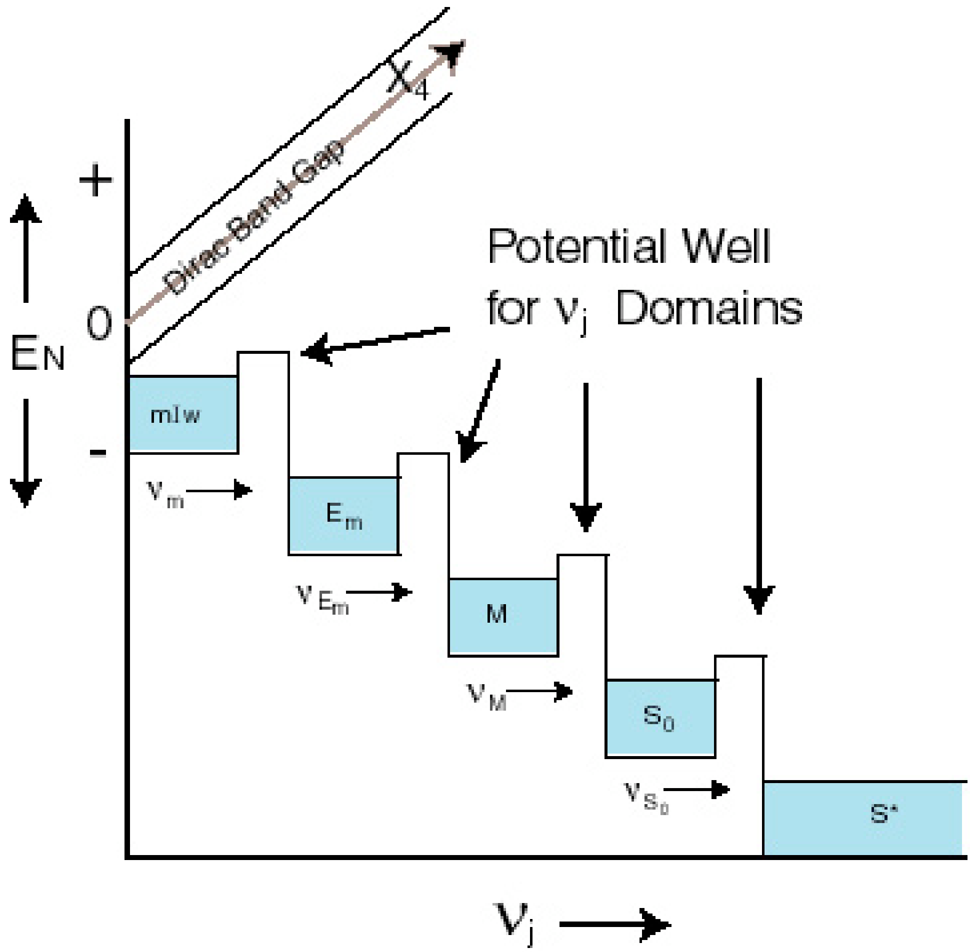

Figure 3b. Energy band diagram within a high spirit thermodynamic potential well.

In contrasting the torsion model and the Tiller Model, the former is directly proportional to the D-space mass spin density, which is less than the total D-space mass density while the latter can be quite independent of D-space mass density and can be appreciably larger than the D-space mass density. This latter point but not the former is consistent with present-day experimental observations.

D. <u>The Tiller Model Perspective on Attractive vs. Repulsive Forces Associated with Subtle Energies and Phase Transitions.</u>

Our experimental picture will be that of a flat-topped cylindrical vacuum chamber with a torsion pendulum suspended from the top-center of the vacuum chamber. There are two cases to consider. One case is the asymmetric pendulum and the other is the circular disk pendulum; for the former, a small cylindrical vessel containing either acetone or water is placed adjacent to the small mass (a solid sphere of some material for example). For the latter, the vessel of acetone or water is sitting centrally on the flat top of the vacuum chamber immediately on top of the fiber suspension point. For the water case, a cooling mechanism is applied only to that vessel so as to slowly and uniformly cool the entire volume of water to a temperature $T = T_M - \Delta T$ (undercooled by ΔT below the melting temperature of ice, $T_M = 0\ ^oC.$). We presume freezing to be initiated at ΔT uniformly along the bottom surface of the vessel and that a flat ice/water interface moves upwards at a constant velocity, V_I. For the acetone case, a heating mechanism is applied only to that vessel so as to slowly and uniformly heat the entire volume of water to a temperature $T = T_B + \Delta T$ (superheat by ΔT above the boiling temperature of acetone, $T_B = 56\ ^oC.$). We presume the evaporation of acetone to occur uniformly along the upper surface of the water and that a water/vapor interface moves downwards at a constant velocity, V_A.

Figure 4 provides schematic plots of chemical potential, μ, as a function of temperature, T, in the immediate region of the transformation temperature T_T, for the two concerned phases. Assuming thermodynamic equilibrium at the transforming interface, all

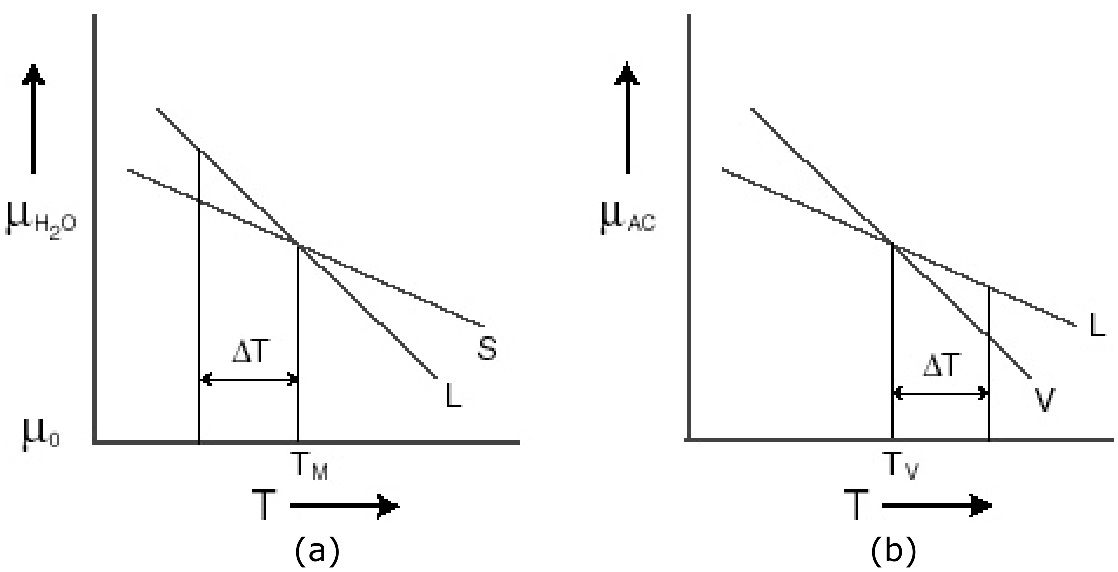

Figure 4. Schematic, approximate plots of thermodynamic chemical potential, μ, for (a) the H_2O liquid to solid transformation at T_M-ΔT and (b) the acetone liquid to vapor transformation at T_V+ΔT.

of the thermodynamic driving force, ΔG, for the phase transformation is consumed via the details of the heat transformation process[6]. Because of convection, the steady state, one-dimensional, temperature distributions attached to the transforming interface, are given by:

Water Freezing (see Figure 5a)

$$T_L - T_\infty \approx \Delta T\left(1 - \frac{x}{\delta_L}\right); \quad \Delta T = T_M - T_\infty \tag{1a}$$

Here, T_∞ is the far-field temperature of the bulk liquid at $x \geq \delta_L$. T_M is the ice/water interface temperature, V_T is the velocity of the interface moving in the x-direction (x=0 at the interface) and δ_L is the liquid convective boundary layer thickness at the ice-water interface. Here, V_I is given by

$$V_I = \frac{-K_L}{\Delta H_F}\left(\frac{\partial T_L}{\partial x}\right)_0 = \frac{K_L \Delta T}{\Delta H_F \delta_L} \tag{1b}$$

where K_L is the thermal conductivity of the water (1.44 x10^{-3} cal/sec ^{o}C. cm) and ΔH_F is the latent heat of fusion (cal/cm^3). In this case, the entropy production, ΔS_I is given by

$$\Delta S_I = \frac{-A_I t V_I \left|\Delta H_F\right|}{T_M} \tag{1c}$$

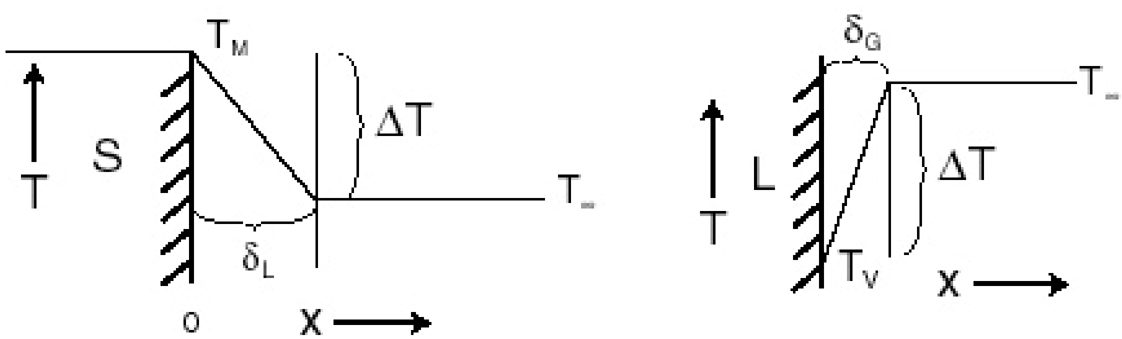

(a) (b)

Figure 5. Approximate temperature distributions for (a) the freezing of water to form ice and (b) the evaporation of acetone to form H_3C_6O molecular vapor.

where A_I is the area of the ice/water interface and t is time. Since the entropy carried by the interface is a steady state process given approximately by $\delta S \approx C_P \Delta T/(T_M - 1/2\Delta T)$, it can be neglected ($C_p$ is the specific heat of the water at constant pressure and $\delta S << \Delta S_I$).

Acetone Evaporation (see Figure 5b)

$$T_g - T_V \approx \Delta T\left(\frac{x}{\delta_g}\right); \quad \Delta T = T_\infty - T_V \tag{2a}$$

Here, Tg is the gas temperature, T_V is the vaporization temperature (T_V ~ 56 ^oC.), T_∞ is the far field temperature and δ_g is the gas phase convective boundary layer thickness at the liquid/gas interface. Here, V_g is given by

$$V_g = \frac{-K_g}{\Delta H_V}\left(\frac{\partial T_g}{\partial x}\right)_0 \approx \frac{-K_g \Delta T}{|\Delta H_V|\delta_g} \tag{2b}$$

where ΔH_V is the heat of vaporization. In this case, the entropy production, ΔS_A, is given by

$$\Delta S_A = \frac{A_A t |V_G||\Delta H_V|}{T_V} \tag{2c}$$

In both cases, Equations 1c and 2c grow linearly with time with ΔS_A having a positive coefficient while ΔS_I has a negative coefficient. These are both D-space properties and have an **absolutely negligible** force effect on the small spherical mass or the disk-suspending fiber inside the vacuum chamber. However, for the R-space counterparts to ΔS_I and ΔS_A, that is another story.

Evaluating the R-space-Counterparts and Interactions

For any D-space time-dependent property, **ΔS(t)** for example, one first calculates its equilibrium R-space counterpart via use of the deltron-modulated Fourier Transform procedure described via Equations 4 in White Paper VII[(4)]. In particular, we use

$$g\left(k_t\right)=\frac{1}{\left(2\pi\right)^{1/2}}\int_{-\infty}^{\infty} C_\delta\left(t,k_t\right)\Delta S(t)\, e^{i2\pi t\bullet k_t} dt \tag{3a}$$

In the zeroth order approximation, the unknown function, $C_\delta(t,k_t)$, in Equation 3a just becomes the constant term, α_{eff}, utilized regularly in this series of White Papers, i.e.,

$$g\left(k_t\right)\approx\frac{\alpha_{eff}}{\left(2\pi\right)^{1/2}}\int_{-\infty}^{\infty} Bt\ e^{i2\pi t\bullet k_t} dt \tag{3b}$$

where B is either $-A_I V_I|\Delta H_F|/T_M$ or $A_A|V_G \Delta H_F|/T_V$ which are both constants and can be brought out from under the integral sign. Thus, we find that

$$g\left(k_t\right)\approx\frac{\alpha_{eff}B}{\left(2\pi\right)^{1/2}}\int_{-\infty}^{\infty} t\ e^{at} dt \quad \text{where } a = 2\pi i k_t = ia' \tag{3c}$$

$$\approx\frac{\alpha_{eff}B}{\left(2\pi\right)^{1/2}}\left[\frac{e^{at}}{a^2}\left(at-1\right)\right]_0^{t*} \tag{3d}$$

$$\approx\frac{-\alpha_{eff}B}{\left(2\pi\right)^{5/2}k_t^2}\left\{e^{2\pi i k_t t*}\left(2\pi i k_t t^*-1\right)+1\right\} \tag{3e}$$

From Equation 3e, one can see that it contains both mathematically real and imaginary parts. For this reason, it is also useful to express this result in phasor notation which uses the following format

$$g\left(k_t\right)=R\left(k_t\right)e^{i\theta\left(k_t\right)} \tag{4a}$$

Here, R is the magnetic information wave amplitude as a function of wave number, k_t, and θ is the phase of the wave as a function of k_t. The Equation 4a relationship can be simply illustrated pictorially via Figure 6.

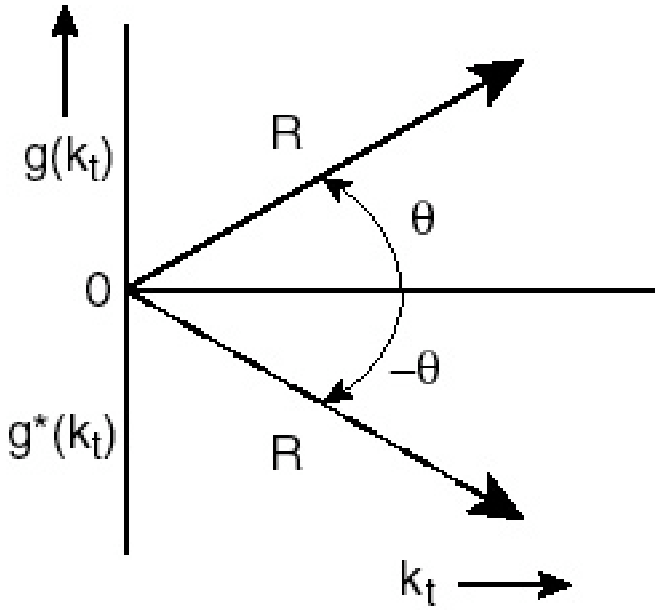

Figure 6. A schematic representation of the phasor format for the vector $g(k_t)$ and its complex conjugate $g^*(k_t)$.

To obtain the amplitude, R, also called the modulus, one must take the square root of the product $g(k_t)g^*(k_t)$. If one wishes to obtain the R-space energetic contribution, Q_m, from this information wave conjugate, one must integrate the wave intensity, $I(k_t) = R^2(k_t)$, over all of k_t-space (R-space) to obtain Q_m. Using Equation 3e and the definition of $I(k_t)$, we can calculate the following

$$I(k_t) = \left(\frac{\beta}{k_t^2}\right)^2 \left\{2 + \left(a't^*\right)^2 - 2\left[a't^* \sin\left(a't^*\right) + \cos\left(a't^*\right)\right]\right\} \quad (4b)$$

where

$$\beta = \frac{-\alpha_{eff} B}{\left(2\pi\right)^{5/2}} \quad and\ a = ia' \quad (4c)$$

and

$$Q_m = \int I\left(k_t\right) dk_t \quad (4d)$$

For the current example, we need to do something a little different because we are seeking to evaluate the R-space interaction between the $g(k_t)$ vector from Equation 3c and the R-space conjugate vectors for (a) the entropy for the small spherical mass inside the vacuum chamber relative to its D-space mass centroid. These are vector addition issues and require that the same mass centroid be used for all the vectors involved in the interaction. In case (a), this involves just a translation process of either the evaporating acetone centroid or the freezing water centroid to the position of the sphere centroid. In case (b), it is a little more complicated because (i) the fiber/disk torsion system needs to be separated into two parts, the fiber itself and the disk itself, (ii) one part requires its centroid to be translated to the centroid of the other (the disk to the fiber centroid) and (iii) a rotation of an angle ϕ is involved so this aspect of the coordinate system change must also be accounted for.

For any D-space object, its translation from its centroid coordinates of (0,0,0) to the new position coordinates of $(\bar{x},\bar{y},\bar{z})$ yields[7], for the change from $g(k_x,k_y,k_z)$ to $g'(k_x,k_y,k_z)$

$$g'\left(k_x,k_y,k_z\right)=e^{i\left(\bar{x}k_x+\bar{y}k_y+\bar{z}k_z\right)}g\left(k_x,k_y,k_z\right) \tag{5a}$$

If the D-space object also involves a rotation in a plane by an angle ϕ, then $g'(k_x,k_y,k_z)$ must also be changed to $g''(k'_x,k'_y,k'_z)$ to account for the x-y planal rotation by angle ϕ. It is interesting to speculate on events wherein differences in time, t, need to be considered. In such a case, one must translate t into a fourth distance coordinate $x_4=iv^*t$, where $v^*=c$, the velocity of light in Einstein's relativity considerations, then the RHS of Equation 5a must be multiplied by $\exp[iv^*\Delta t k_t]$. For the $g''(k'_x,k'_y,k'_z)$ case, we must use

$$k'_x = k_x\cos\phi+k_y\sin\phi \; ; \; k'_y = -k_x\sin\phi+k_y\cos\phi. \tag{5b}$$

For a solid sphere of radius, R, centered at (0,0,0), it has a volume of $(4/3)\pi R^3$ and, because of its symmetry about the coordinate (0,0,0), $g(k_r)$ is mathematically real and it can be shown that, the normalized modulus, I_n, is given by

$$I_n\left(k\right)=\frac{g\left(k_r\right)}{\frac{4}{3}\pi R^3}=\frac{3}{4\pi R^3}\left|\frac{4\pi}{k_r^3}\left[\sin\left(k_rR\right)-k_rR\cos\left(k_rR\right)\right]\right|, \tag{6a}$$

where

$$k_r=\left[k_x^2+k_y^2+k_z^2\right]^{1/2}. \tag{6b}$$

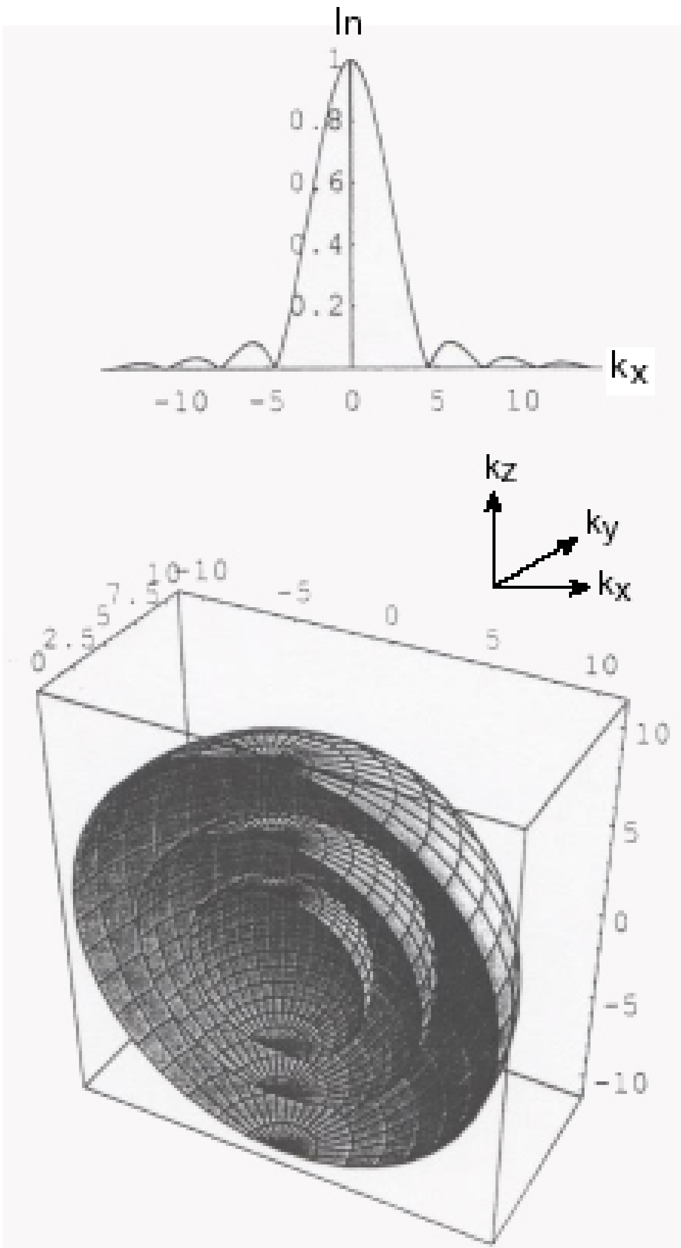

Figure 7. For a full sphere, a cross-sectional view for In (k_x,0,0) and the first three concentric shells obtained for the normalized isomodulus. By symmetry, In(K_x,0,0) = In(0,K_y,0 = In(0,0,k_z).

Figure 7, shows that $I_n(k_r)$ consists of a series of concentric spheres with a cross-section having a large peak centered at (0,0,0) and several much smaller decaying peaks as r increases toward R.

To evaluate the interaction between the R-space entropy conjugate of the small mass sphere inside the vacuum chamber with the R-space entropy conjugate of either the water freezing vessel or the acetone evaporation vessel located outside the vacuum chamber, we must use the Equation 3e formula modified by the Equation 5a factor to obtain for the system of two vectors, $g_S(k_t)$, shown in Equation 7 as

$$g_S(k_t) = \gamma g_{Sphere}(k_t) + g'_{vessel}(k_t). \quad (7a)$$

Here, γ is the constant thermodynamic entropy per unit volume value for the D-space sphere and g'_{vessel} is Equation 3c modified according to Equation 5a. If $g_S(k_t)$ is greater than $\gamma g_{Sphere}(k_t)$ then the vectors add which means that the non-local force is attractive. If instead, $g_S(k_t)$ is less than $\gamma g_{Sphere}(k_t)$, the two vectors subtract and a repulsive force is operating. The difficulty we have in making a final evaluation is that although the parameter B switches from being negative for the freezing water case to positive for the evaporating acetone case, α_{eff} can in general be of a mathematically complex form, $\alpha_{eff} = \alpha_0 + i\alpha_1$, with the coefficients either positive or negative and we have no experimental data to decide which is operational in either case. However, our present experience has only dealt with cases that α_{eff} is mathematically real and positive in magnitude. All that can be positively stated at this time is that the sign of the second term in Equation 7a is of opposite sign for the water freezing case than for the acetone evaporation case so that one is attractive in form (the $\alpha_{eff} > 0$ case) while the other is repulsive in form (the $\alpha_{eff} < 0$ case). This is in internal self-consistency with the Kosyrev experimental findings and tells us something about what α_{eff} must be.

Turning to item 3 of the introduction, we follow the same procedure as for item 2. Here, Equations 3e, 4 and 5 still hold. However, now, we must evaluate the counter part to Equations 6 for the torsion-disk pendulum which has two distinctive parts (1) the fiber of length L and radius r and (2) the flat disk of radius R and thickness, δ, hanging at the end of the fiber. In this case, not only must we evaluate $g(k_x,k_y,k_z)$ relative to its own centroid for the two parts, but we must also evaluate the equation 5a factor and the Equation 5b factor. Although we will ultimately end up with the lack of knowledge of the details involved with $\alpha_{eff} = \alpha_0 + i\alpha_1$, it is pedagogically useful to learn what is actually involved in trying to compare the experimental data with the Tiller Perspective theoretical predictions.

For item 3 of the introduction, the torsion pendulum is a system of two parts, (a) a fiber of length L, aligned in the z-direction, with thickness x_0 and y_0 plus (b) a thin solid disk of radius R perpendicular to the fiber. The D-space centroid of the latter must be displaced upwards by a distance L/2 while that of the vessel of the freezing water or evaporating acetone must be displaced downwards by a distance L/2. Further, allowance must be made for a circular rotation in the plane of the disk by an angle $\pm\,\phi$.

Relative to their own centroids[7], we have

(a) Fiber (see Figure 8)

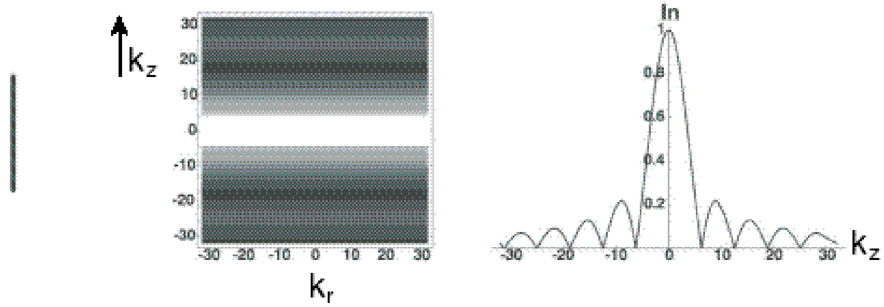

Figure 8. A (k_z, k_r) normalized modulus map in the middle and kz-section profile on the right for the vertical fiber of length, L, on the left.

$$g_F\left(k_x,k_y,k_z\right)=\frac{\alpha_{eff}}{\left(2\pi\right)^{1/2}}\frac{\sin\left(k_zL/2\right)}{k_z/2}e^{ik_xx_0}e^{ik_yy_0} \qquad (7a)$$

(b) Disk (see Figure 9)

$$g_D\left(k_x,k_y,k_z\right)=\frac{\alpha_{eff}2\pi R}{k_r}J_1\left(k_rR\right)e^{ik_zz_0} \qquad (7b)$$

with $k_r=\left[k_x^2+k_y^2\right]^{1/2}$
and J_1 is the Bessel function of order one and

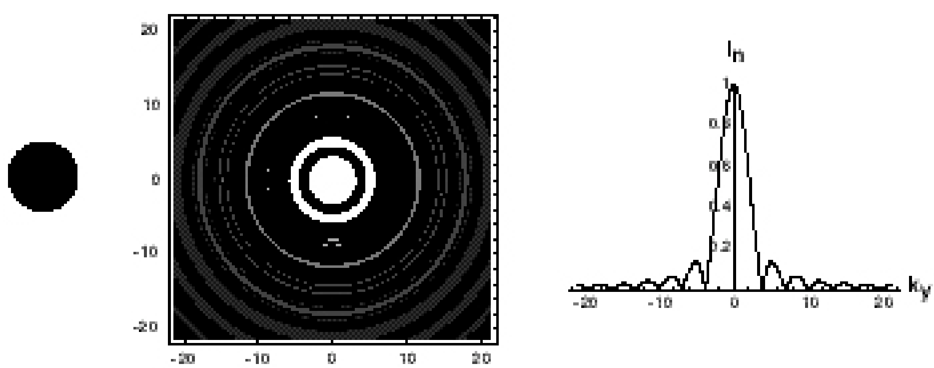

Figure 9. (x,y) planar and cross-sectional plots of normalized modulus, I_n, for a thin circular disk.

(c) Vessel

$$g_V\left(k_r,k_z,k_t\right)=\frac{4\pi\alpha_{eff}RJ_1\left(k_rR\right)}{k_rk_z}\sin\left(k_zH/2\right)g\left(k_t\right) \tag{7c}$$

where H is the height of the cylindrical vessel and R is its radius. For the entire system, $g_S(k_x,k_y,k_z)$ is given by

$$\begin{aligned} g_S\left(k_x,k_y,k_z,k_t\right)&=\gamma_F g_F\left(k_x',k_y',k_z\right)+\gamma_D e^{iLk_z/2}g_D\left(k_x',k_y',k_z\right)\\ &+e^{-iLk_z/2}g_V\left(k_r,k_z,k_t\right)\end{aligned} \tag{8a}$$

with

$$\begin{aligned} k_x' &= k_x\cos\phi+k_y\sin\phi\\ k_y' &= -k_x\sin\phi+k_y\cos\phi\end{aligned} \tag{8b}$$

and γ_F, γ_D are the entropic content of the fiber and disk, respectively. Here, the torque strain energy in the fiber due to rotation by the angle ϕ has been neglected. For a system of radial symmetry, it can be readily shown that $k'_r=k_r$ and that a $+\phi$ rotation produces the same result as a $-\phi$ rotation; thus, the only difference that enters the above Equation for g_S is the sign reversal of the parameter B that enters g_V.

Summing Up and Closing Comments

1. The torsion perspective is to accept the orthodox view of spin and go on from there. The psychoenergetic science perspective is to explain where spin comes from in terms of its duplex space model.

2. The torsion perspective on Dark Matter is that electric particle spin introduces a new term (small in magnitude) into Einstein's gravitational equations. It is a new effect but smaller in magnitude than the normal, electric particle mass effect in nature. This is at variance with the experimental observation that the gravity effect associated with Dark matter is several times greater than the collective electric atom/molecule gravitational effect.

   The psychoenergetic science Dark Matter effect is based on the proposed existence of negative energy, faster than EM light, magnetic information wave substance functioning in the physical vacuum domains of nature. This leads to negative mass substance interacting with other negative mass substance leading to an invisible positive gravity type of effect. The magnitude of this effect is not limited by the density of electric substance-created gravity so the former can be significantly greater in magnitude than the latter.

3. The torsion perspective on Dark Energy is associated with the spin-altered energy states of electric atom/molecule substance leading to enhanced EM radiation emission relative to non-spin related EM emission. All of these EM emissions produce space curvature effects and thus gravitational effects. However, in general, the spin-related EM photon energies are significantly smaller in magnitude than those associated with inter-shell, electric atom/molecule emissions. Thus, it is likely that the spin-related photon space curvature changes are appreciably less than the normal, non-spin-related photon space curvature changes. Even for average temperatures of $\sim 2^o - 3^o$ Kelvin, the spin-related photon emission, space curvature effects are not larger than the normal electric atom/molecule space curvature effects.

   The psychoenergetic science Dark Energy effect is due to magnetoelectric (ME) photon emission from magnetic information wave substance functioning in the physical vacuum. These have been proposed to be several orders of magnitude larger than normal EM radiation energies and are traveling faster than EM light so as to produce large Dark Energy effects.

4. The torsion perspective only increases slightly the rate of gravitationally-induced deceleration of planets and stars at the outer envelope of our expanding cosmos. It does not account for the experimentally observed acceleration.

   The psychoenergetic science perspective, on the other hand, allows for a shift from deceleration to acceleration when a sufficient cosmic deltron population exists to allow slower than v=c, positive mass, EM substance to interact with faster than v=c, negative mass, ME substance so that a gravitational repulsion occurs between the Dark matter/Dark energy substance of the inner regions of the cosmos with electric atom/molecule substance of the outermost envelope of the cosmos.

5. With respect to the repulsive force on the small mass end of the asymmetric pendulum associated with an external vessel of evaporating acetone versus an external vessel of freezing water, both the torsion perspective and the psychoenergetic science perspective predict an opposite sign of force for the two cases based upon entropic considerations (rate of entropy production).

6. With respect to clockwise vs. counterclockwise rotation of the torsion pendulum experiment with acetone evaoporation versus water freezing, both the torsion perspective and the psychoenergetic science perspective predict an opposite sign of rotation for the two cases. However, our present-day lack of quantitative information on the "deltron modulation function" in the psychoenergetic science perspective inhibits one from stating which sign of rotation goes with which vessel. At present we are limited to using only the zeroth order of approximation (the α_{eff} -approach to solving the important integrals).

7. In terms of the basic philosophical perspective that entropy production rate and time are somehow fundamentally connected in nature, one might speculate that perhaps a Heisenberg uncertainty condition is involved. However, when one compares the units of $\Delta S \Delta T$ (erg/^{o}C) and Planck's constant, h, (erg sec), one sees a real inconsistency. Thus, if there is such a fundamental relationship in nature, the path to proving it is not obvious.

References

1. C. Swanson, Life Force: The Scientific Basis (Poseidia Press, Tucson, AZ, 2009).
2. W. A. Tiller, "Towards a Medicine of Subtle Energies" in Holistic Dimensions in Healing (A Resource Guide), Ed.: L. Kaslov (Doubleday-Dolphin Press, 1977).
3. W. A. Tiller, "What are Subtle Energies?" *Journal of Scientific Exploration,* 7 (1993) 293.
4. W. A. Tiller, "Why We Need to Create a New Reference Frame (RF) for Viewing Nature and How Do We Do It? (see www.tiller.org; White paper VII, March, 2009).

5. W. A. Tiller, "What Does the Dirac Negative Energy Sea Mean and Why Has Today's Orthodox Physics Neglected It? (see www.tiller.org; White paper VI, March, 2009).
6. W. A. Tiller, The Science of Crystallization: Microscopic Interfacial Phenomena, (Cambridge University Press, New York, N.Y., 1991, Chs 1 and 6 pp 232-233).
7. W. A. Tiller , W. E. Dibble, Jr and M. J. Kohane Conscious Acts of Creation: The Emergence of a New Physics (Pavior Publishing, Walnut Creek, CA, 2001, pp 253-261 and pp 304-309).

